Formation and growth mechanism of thin Cu_6Sn_5 films in Sn/Cu and Sn-0.1AlN/Cu structures using laser heating

Zhang Liang
School of Materials Science and Engineering, Xiamen University of Technology, Xiamen, China and
School of Mechatronic Engineering, Jiangsu Normal University, Xuzhou, China

Abstract

Purpose – The purpose of this study is the formation and growth of nanoscale intermetallic compounds (IMCs) when laser is used as a heat source to form solder joints.

Design/methodology/approach – This study investigates the Sn/Cu and Sn-0.1AlN/Cu structure using laser soldering under different laser power: (200, 225 and 250 W) and heating time: (2, 3 and 4 s).

Findings – The results show clearly that the formation of nano-Cu_6Sn_5 films is feasible in the laser heating (200 W and 2 s) with Sn/Cu and Sn-0.1AlN/Cu system. The nano-Cu_6Sn_5 films with thickness of 500 nm and grains with 700 nm are generally parallel to the Cu surface with Sn-0.1AlN. Both IMC films thickness of Sn/Cu and Sn-0.1AlN/Cu solder joints gradually increased from 524.2 to 2025.8 nm as the laser heating time and the laser power extended. Nevertheless, doping AlN nanoparticles can slow down the growth rate of Cu_6Sn_5 films in Sn solder joints due to its adsorption.

Originality/value – The formation of nano-Cu_6Sn_5 films using laser heating can provide a new method for nanofilm development to realize the metallurgical interconnection in electronic packaging.

Keywords Intermetallic compounds, Laser heating, Solder joints, Nano-Cu_6Sn_5 films, AlN nanoparticles

Paper type Research paper

1. Introduction

Cu metal has been used in electronic packaging field for lead-frame and pad on substrate due to the high strength, electrical conductivity, thermal conductivity and good processability. To establish a connection between the lead or pad and the device, Sn metals with outstanding mechanical performance have become the primary connection material for electronic interconnection. This is owing to their ability to react with Cu, forming IMCs that facilitate metallurgical bonding (Hu *et al.*, 2021; Liu *et al.*, 2021). Due to the brittle performance of IMCs, cracks initiated and propagated in excessively thick IMC layer in service leading to early solder joint failure (Zhang *et al.*, 2021; Wang *et al.*, 2022). Therefore, controlling the thickness of IMCs at Cu interface has become an important research topic in the field of electronic packaging.

Laser heating with high energy density laser beam as heat source is an efficient and precise soldering method. Laser-soldered lead-free solder can reduce the heating time and rapidly form solder joints, which can induce a thinner IMCs layer. There is a literature (Kunwar *et al.*, 2020) investigated the interfacial Cu_6Sn_5 IMC in Sn-*x*Ag-*y*Cu/Cu structure, the morphology of IMC can be observed with types-prismatic and scalloped, which can be influenced by the laser power, scan speed and composition. Nishikawa and Iwata (2015) have investigated the IMC layer growth at Sn-3.0Ag-0.5Cu/Cu interface after laser soldering and isothermal aging. It is found that a relatively thin Cu_6Sn_5 layer is formed at the interface after laser soldering. The mechanical performance of the solder joints under laser soldering at 20 W for 40 s is superior to that of solder joints under reflowing. Huan *et al.* (2022) have studied the laser soldering of 8-SOIC to analyze the interfacial reaction between Sn-3.0Ag-0.5Cu and Cu or Ni/Al, the results indicate that the IMC thickness is less than 5 μm near Cu, the IMC thickness is less than 1 μm near Ni/Al. Abdullah and Idris (2021) have studied the IMC growth of Sn-*x*Cu/ENIG (electroless nickel immersion gold) solder by laser soldering. The result shows that the IMC layer thickens while the equilibrium contact angle reduces with the amount of Cu increasing, and Sn-0.7Cu/ENIG exhibits more excellent performance as compared to other content of Cu. Liu *et al.* (2010) investigated the effect of the temperature of protection atmosphere on morphology of IMCs in laser reflowed Sn-2.0Ag-0.75Cu-3.0Bi solder joints. The results indicate that the needle-like $AuSn_4$ IMC and Au-rich phases were

---

The current issue and full text archive of this journal is available on Emerald Insight at: **https://www.emerald.com/insight/0954-0911.htm**

Soldering & Surface Mount Technology
36/5 (2024) 268–275

[ISSN 0954-0911]
[DOI 10.1108/SSMT-05-2023-0021]

This work was financially supported by Fujian Provincial “Minjiang Scholar” Distinguished Professor Talent Plan Project, Henan Provincial Distinguished Researcher Project and Natural Science Foundation of Jiangsu Province Project (BK20211351).

Received 5 May 2023
Revised 15 June 2023
2 January 2024
14 January 2024
4 February 2024
Accepted 6 February 2024

Figure 1 Experimental procedure for nanothin Cu_6Sn_5 film formation

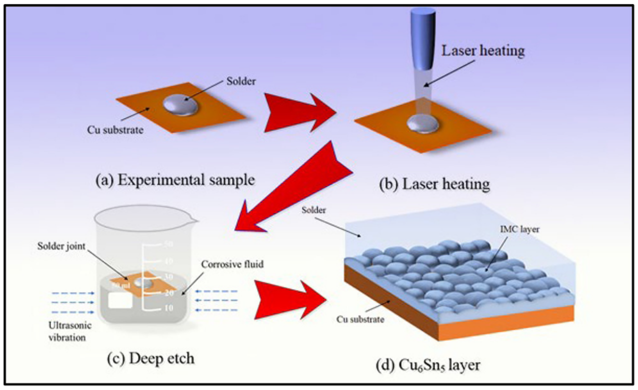

Source: Authors' own work

formed in Sn-2.0Ag-0.75Cu-3.0 Bi solder joint protected by N_2 atmosphere at room temperature. When the temperature was upper 100°C, the Au-rich phases almost disappeared, and orientation of the needle-like $AuSn_4$ IMCs changed obviously. Thus, the morphology of Au-Sn IMCs in the laser reflowed solder joints can be controlled by regulating N_2 atmosphere temperature. But until now, there is no detailed report on the study of laser heating inducing the formation of nanothin IMC layer.

In this paper, we fabricate the Sn/Cu and Sn-0.1AlN/Cu solder joints using laser soldering. The effect of laser power and heating time on the thickness of Cu_6Sn_5 layer and sizes of Cu_6Sn_5 grains with Sn/Cu and Sn-0.1AlN structures was investigated systematically. The objective is to establish a correction between nano-Cu_6Sn_5 films and laser parameters/AlN additives. A new method to enhance the reliability of solder joints on Cu substrate in electronic packaging is also aimed to be explored.

2. Experiment

In this study, the Sn-AlN composite solder comprising Sn paste and reinforcing AlN particles with an average diameter ranging from 30 to 50 nm was used. The composite solder was fabricated by ultrasonic agitation to ensure the uniform distribution of nanoparticles in matrix. Solder paste (approximately 0.2 g) was put on the Cu substrate (25 mm × 25 mm × 0.5 mm) cleaned with C_2H_5OH solution. Then the laser heating under different

Figure 2 Surface morphologies of Cu_6Sn_5 films on Sn/Cu interface with different laser parameters

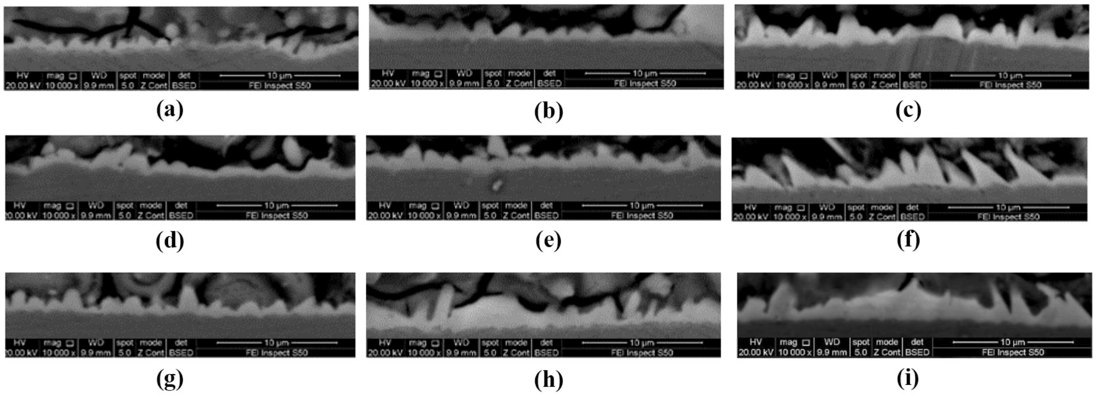
(a) (b) (c)
(d) (e) (f)
(g) (h) (i)

Notes: (a) 200 W and 2 s; (b) 200 W and 3 s; (c) 200 W and 4 s; (d) 225 W and 2 s; (e) 225 W and 3 s; (f) 225 W and 4 s; (g) 250 W and 2 s; (h) 250 W and 3 s; (i) 250 W and 4 s
Source: Authors' own work

Figure 3 Surface morphologies of Cu_6Sn_5 films on Sn-0.1AlN/Cu interface with different laser parameters

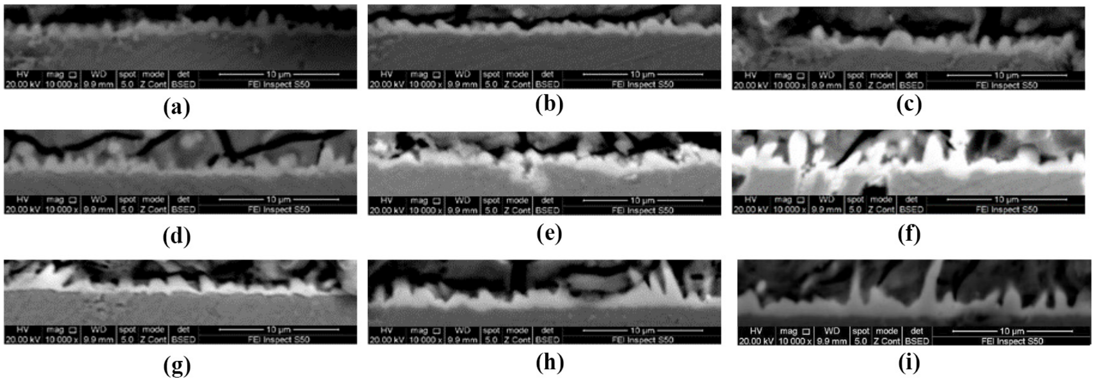
(a) (b) (c)
(d) (e) (f)
(g) (h) (i)

Notes: (a) 200 W and 2 s; (b) 200 W and 3 s; (c) 200 W and 4 s; (d) 225 W and 2 s; (e) 225 W and 3 s; (f) 225 W and 4 s; (g) 250 W and 2 s; (h) 250 W and 3 s; (i) 250 W and 4 s
Source: Authors' own work

Figure 4 IMC thickness with different laser power and heating time

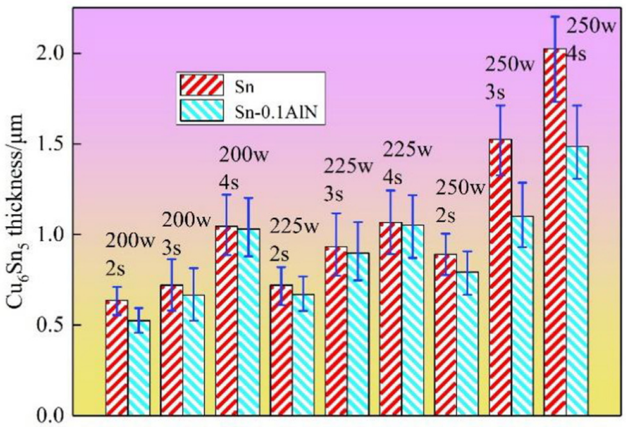

Notes: The process parameters from left to right are: 200 W, 2 s; 200 W, 3 s; 200 W, 4 s; 225 W, 2 s; 225 W, 3 s; 225 W, 4 s; 250 W, 2 s; 250 W, 4 s; 250 W, 4 s
Source: Authors' own work

laser power (200, 225 and 250 W) and heating time (2, 3 and 4 s) was used to form molten solder to react with Cu substrate as shown in Figure 1, after laser heating, 25%HNO_3 and 75% C_2H_5OH mixed solution were selected for the deep etching to prepare samples, the scanning electron microscope (SEM) and transmission electron microscope (TEM) were used to observe the morphologies of nanothin IMC layer and IMC grains. To minimize experimental errors, every composite with ten samples was selected for observation and the average value was taken.

3. Results and discussions

The interfacial structure of Sn/Cu solder joints prepared at different laser powers (200, 225 and 250 W) and heating times (2, 3 and 4 s) is shown in Figure 2. The scallop-type Cu_6Sn_5 intermetallic compound layer can be observed parallel to the Cu substrate, it is evident that thickness of Cu_6Sn_5 layer from 635.6 to 890.9 nm is increasing with the increase of laser power from 200 to 250 W for 2 s heating time. Moreover, the scallop-type Cu_6Sn_5 grains with several microns in height during solid–liquid interdiffusion reaction can also be obtained in

Figure 5 Surface morphologies of Cu_6Sn_5 films on Sn/Cu interface with different laser parameters

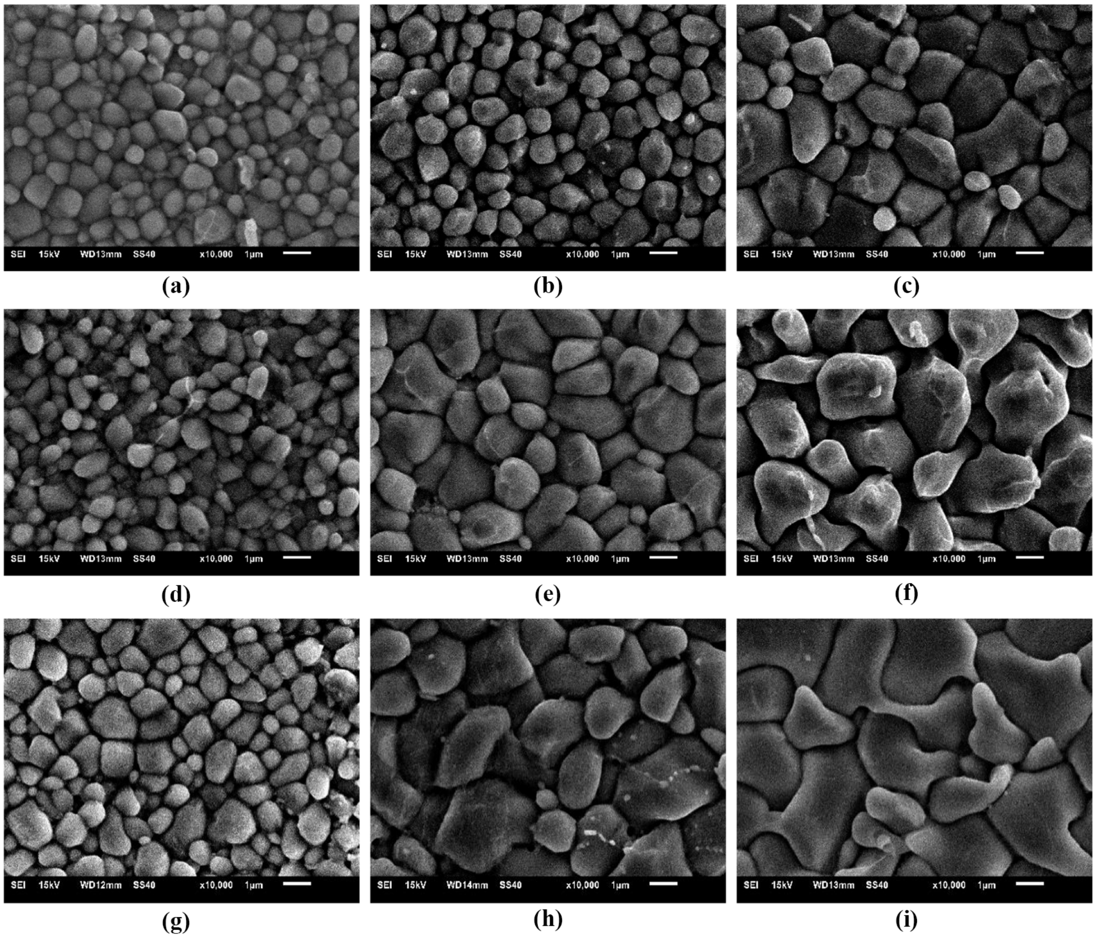

Notes: (a) 200 W and 2 s; (b) 200 W and 3 s; (c) 200 W and 4 s; (d) 225 W and 2 s; (e) 225 W and 3 s; (f) 225 W and 4 s; (g) 250 W and 2 s; (h) 250 W and 3 s; (i) 250 W and 4 s
Source: Authors' own work

Cu/Sn-Ag/Cu structure with about 10 μm thickness solder (Gusak *et al.*, 2020). Comparing with the influence of laser power, the influence of heating time is more intense, for 200 W laser soldering, it can be seen that the thickness of Cu_6Sn_5 layer grows from 635.6 to 1045.3 nm, as shown in Figure 2(a)–(c), which induce 1.64 times as heating times from 2 to 4 s. Moreover, when the laser power reaches 225 W, the Cu_6Sn_5 film is turned into needle-like structures and the Cu_6Sn_5 thickness increases from 720 to 1066.5 nm while the laser heating time rises from 2 to 4 s in Figure 2(d)–(f). As the laser power rises to 250 W, the growth rate of Cu_6Sn_5 films has increased significantly and the scallop-shaped Cu_6Sn_5 films are connected to form flake IMCs, as shown in Figure 2(g)–(i). The thickness of Cu_6Sn_5 films is increased to 2025.8 nm when the laser heating rise to 4 s. Thus, the Cu_6Sn_5 films thicken with the laser power or heating time extending.

Figure 3 shows the SEM morphologies of Sn-0.1AlN/Cu solder suffered laser heating (2, 3 and 4 s) under different laser power (200, 225 and 250 W). Likewise, it is found that the typical scallop-shaped Cu_6Sn_5 films at the Sn-0.1AlN interfacial surface and the IMC films get thicker as the laser heating time or power increased. After the laser heating time added from 2 to 4 s, the Cu_6Sn_5 films thickness of Sn-0.1AlN solder at 200 W increases from 524.2 to 1030 nm, as shown in Figure 3(a)–(c), which has a decrease of 1.5%–17.5% compared with Sn solder heated from 2 to 4 s. Under 225 W of laser power, the thickness of Cu_6Sn_5 films rises from 668.5 to 1050.9 nm with laser heating from 2 to 4 s, as can be seen in Figure 3(d)–(f), which is 1.5%–7.2% less than that of Sn solder under corresponding condition. When the laser power reaches 250 W, the Cu_6Sn_5 films thickness of Sn-0.1AlN composite solder heated for 2 and 4 s adds up to 792.3 and 1486.1 nm as shown in Figure 3(g)–(i), with a decrease of 11.1%–26.7% by compared with Sn solder under lasering heating for 2 and 4 s. By comparing and analyzing the interfacial thickness of two kinds of structures. It is found that the interfacial thickness of Sn-AlN/Cu is significantly smaller than that of Sn/Cu. The decrease ranged from 1.5% to 26.7%.

The molten Sn expands under laser heating on Cu surface, the increase of laser power will induce the increase of soldering

Figure 6 Surface morphologies of Cu_6Sn_5 films on Sn-0.1AlN/Cu interface with different laser parameters

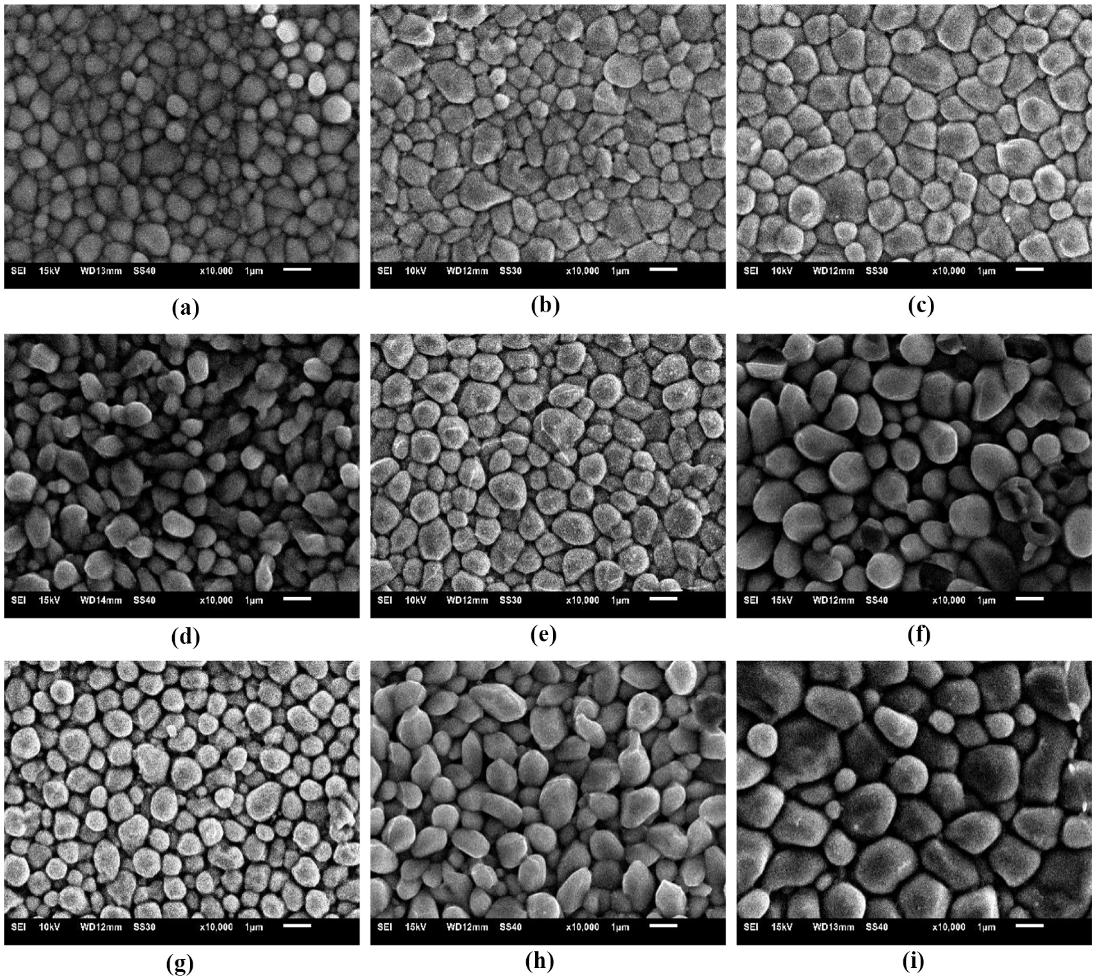

Notes: (a) 200 W and 2 s; (b) 200 W and 3 s; (c) 200 W and 4 s; (d) 225 W and 2 s; (e) 225 W and 3 s; (f) 225 W and 4 s; (g) 250 W and 2 s; (h) 250 W and 3 s; (i) 250 W and 4 s
Source: Authors' own work

temperature, which can enhance the atoms diffusion between Sn and Cu to improve the Cu-Sn reaction. The increase of laser heating time can also improve the atoms diffusion. An appropriate amount of Cu-Sn reaction can form a metallurgical connection, while an excess reaction induces crack initiation and reduces the structure reliability (Li *et al.*, 2021). The IMC thickness of Sn/Cu and Sn-AlN/Cu structures has been obtained by Image-J software, as can be seen in Figure 4. On one hand, both IMC layer thickness of two samples is thin since the heating duration is very short which results in the diffusion. And reaction between molten solder and Cu substrate is insufficient. On the other hand, it is clear that the thickness of Cu_6Sn_5 IMC film of the Sn solder containing AlN nanoparticles is lower than that of pure Sn solder at the same laser soldering condition. Therefore, the nanothin Cu_6Sn_5 films can be found at the Sn/Cu and Sn-AlN/Cu structures at 200 W/225 W with 2 and 3 s, and at 250 W with 2 s.

Figure 7 Cu_6Sn_5 grains diameter with different laser power and heating time

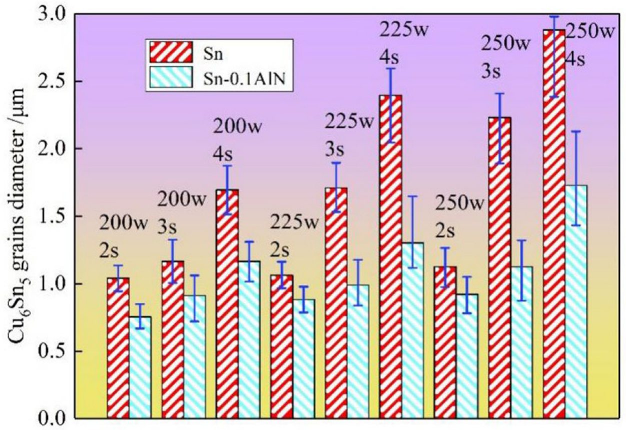

Source: Authors' own work

In addition to the thickness of Cu_6Sn_5 layer being nano-sized, the diameter of Cu_6Sn_5 grains can also reach nanometer size. It is interesting to explore the top view of Cu_6Sn_5 grains, the morphologies of Cu_6Sn_5 grains at Sn/Cu and Sn-0.1AlN/Cu structures with different laser power and heating times are shown in Figures 5 and 6, respectively. The top-view morphologies show that the Cu_6Sn_5 grains grow continuously with the extension of heating time or the increase of laser power. When the laser heating time reaches 4 s, the Cu_6Sn_5 grains in Sn/Cu structure under 250 W of laser power are fused with each other and the Cu_6Sn_5 grain size increases significantly. Figure 7 exhibits the grain diameter of Sn/Cu and Sn-0.1 AlN structure suffered different laser heating time and laser power. It shows that the Cu_6Sn_5 grains sizes in Sn/Cu and Sn-0.1AlN/Cu systems are added along with the laser heating. Under 200 W, the Cu_6Sn_5 grain diameter of Sn-0.1AlN structure heated for 2 s is 752.8 nm, which is less than that (1039.3 nm) of Sn/Cu structure. After heating for 4 s, the Cu_6Sn_5 grain size of Sn-0.1AlN solder is 1164 nm, a decrease of 31.2% compared with that of Sn/Cu. When the laser power rises to 250 W, the diameter of Cu_6Sn_5 grain in Sn/Cu and Sn-0.1AlN/Cu structure heating for 4 s rose to 2877.5 and 1726.5 nm, with an increase of 156% and 87.6% as compared with that of corresponding structure heated for 2 s. The result demonstrates that the growth rate of Cu_6Sn_5 grains in Sn/Cu structure adding with AlN nanoparticles is slower than that without AlN nanoparticles. This exhibits that doping AlN nanoparticles can impede IMC grains growth. Furthermore, the growth of Cu_6Sn_5 grains is controlled by the Cu flux (Xiong *et al.*, 2019). According to Gibbs–Thomson effect (Kim and Tu, 1996), the Cu concentration on the Cu_6Sn_5 grain surface in Sn solder is:

Figure 8 Element mapping of Cu_6Sn_5 film on Sn-0.1AlN/Cu with laser heating (200 W, 1 s)

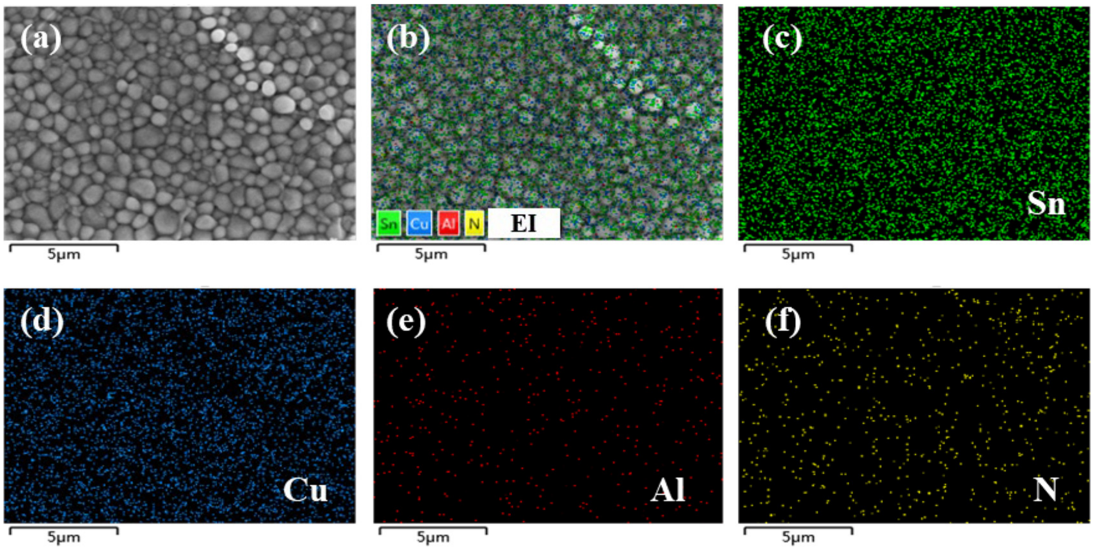

Notes: (a) Overall SEM image; (b) ESD layered image; (c) Sn element; (d) Cu element; (e) Al element; (f) N element
Source: Authors' own work

$$C = C_0 \exp\left(\frac{2\gamma V_m}{rRT}\right) \quad (1)$$

where C_0 is the equilibrium concentration of Cu atoms, γ is the interface energy between molten solder and Cu_6Sn_5 IMC grains, V_m is the molar volume of Cu_6Sn_5 IMC grains, r is the radius of Cu_6Sn_5 IMC grains, R is the gas constant and T is the absolute temperature. Based on Fick's first law (Yao *et al.*, 2017), the maturation flux of Cu is:

$$\mathcal{J}_1 = -D\frac{dc}{dx} \cong -\frac{2\gamma V_m C_0 D}{3\lambda RTr^2}\left(\text{if } \frac{2\gamma V_m}{RTr} 1\right) \quad (2)$$

where D is the diffusion coefficient of Cu, and λ is the dimensionless coefficient. During laser soldering process, the diameter of Cu_6Sn_5 grains is different, and a Cu concentration gradient will exist between the IMC grains, which results in Cu atoms spreading to the large grains from the small ones. Thus, the large grains are growing while the small grains are shrinking. In addition, the diffusion coefficient (D) can be described as follows:

$$D = D_0 \exp\left(-\frac{Q}{RT}\right) \quad (3)$$

Figure 9 TEM of nanothin Cu_6Sn_5 film in Sn-AlN/Cu structure

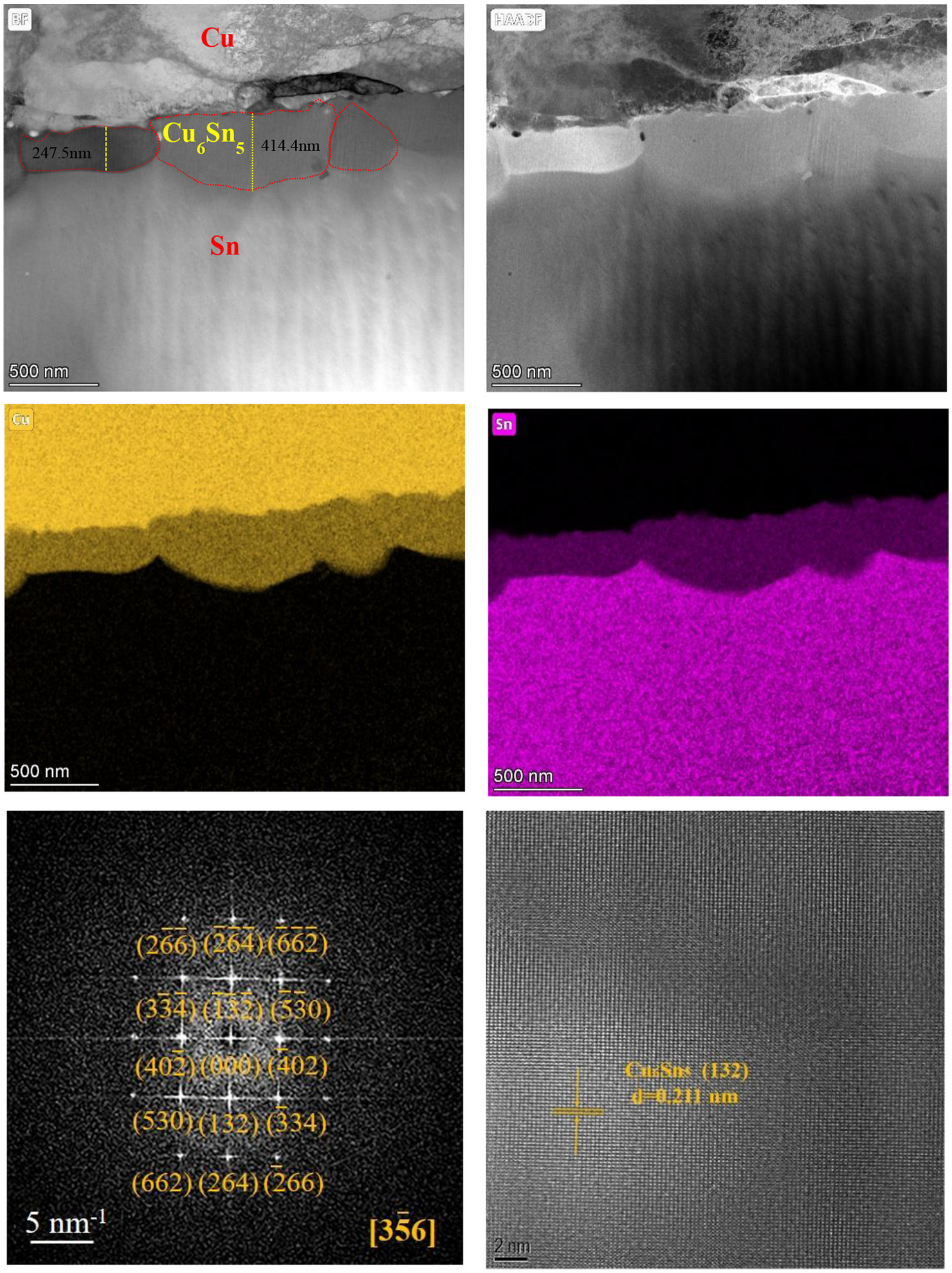

Source: Authors' own work

where D_0 is diffusion constant, and Q is diffusion activation energy. Moreover, the diffusion activation energy represents an atom required to migrate from one place to another place (Sun *et al.*, 2019). The AlN nanoparticles can be adsorbed on the Cu_6Sn_5 grains surface and in the solder matrix, which will impede the diffusion of Cu atoms. Therefore, AlN nanoparticles addition decreases the diffusion coefficient and the diffusion flux ($\mathcal{J}_1$) of Cu atoms, causing the inhibition of IMC growth. Moreover, the element mapping of Sn-AlN/Cu with laser heating for 1 s under 200 W has been obtained, as shown in Figure 8, it is demonstrated that AlN nanoparticles are diffused on the Cu_6Sn_5 grains surface in the Sn-AlN/Cu structure, which represents the AlN nanoparticles absorbed on the grains surface can inhibit the diffusion of Cu and Sn to reduce the Cu_6Sn_5 growth.

To further identify the sizes of nanothin Cu_6Sn_5 film and Cu_6Sn_5 grains, FIB has been used to fabricate ultrathin Sn-AlN/Cu samples, TEM and EDS can be used to observe the elements distribution at the Sn-AlN/Cu interface, as shown in Figure 9. The Cu_6Sn_5 grains can be observed obviously, small Cu_6Sn_5 grains can reach 247.5 nm in height and large grains can reach 414.4 nm in height. The nanothin Cu_6Sn_5 film could enhance the reliability in the future solder joints with 1 μm height in miniature 3D chip stacking. From the HRTEM image of nanothin Cu_6Sn_5, the spacing interplanar measured is 0.211 nm, and identified as Cu_6Sn_5 (132) planar. In the nanothin Cu_6Sn_5 film, no obvious defect, such as Kirkendall voids can be found in this area, only three weeny Kirkendall voids with 30–40 nm diameter can be found. According to the published data from literatures (Vianco *et al.*, 2022), solder joints with different materials, including Sn-Pb/Ni/Au, Sn/Cu and Sn-Ag-Cu/Cu-Ti, have an extensive network of Kirkendall voids formed along the interface, the Kirkendall voids can even 1 μm. Comparing with the published data, we can conclude that the formation of nanothin Cu_6Sn_5 film can enhance the reliability of structure. This further shows that by laser heating, although the heating time is very short, but can obtain a good nanothin Cu_6Sn_5 film on Cu substrate. Nanothin Cu_6Sn_5 films can be used as Cu protective films to improve the reliability of the new generation electronic products.

To further analyze the growth kinetics of nanothin Cu_6Sn_5 film, the relationship between the thickness of IMC (L) and heating time (t) can be expressed by the empirical equation (Liu *et al.*, 2020), as shown in equation (4). In this experiment, the values of L and t can be obtained by measuring the thickness of nanothin Cu_6Sn_5 at different times, based on the logarithm of L and t, the n can be computed to be 0.78 ± 0.29, 0.56 ± 0.05 and 1.15 ± 0.11 for 200, 225 and 250 W in Sn/Cu structure. The n is 1.06 ± 0.29, 0.64 ± 0.05 and 0.93 ± 0.07 for 200, 225 and 250 W in Sn-AlN/Cu structure. From the calculation, it is found that the value of n is significantly larger, more than 0.5, and even up to about 1. In the growth investigation of IMC with prolonged heating (Zhang and Liu, 2020), the value of n is 0.5, it is found that parabolic growth tendency can present the growth of the IMCs growth, but in the present experiment, the thickness of the Cu_6Sn_5 film is nanothin, the thickness of the data is in the initial stage of the parabolic, and is in a very small distance, so the numerical fitting n will close to the linear relationship, as shown in Figure 10. Moreover, with the calculation of D, it is found that the diffusion coefficient is 0.34 ± 0.12, 0.49 ± 0.03 and 0.42 ± 0.06 nm/s^n for 200, 225 and 250 W in Sn/Cu structure, 0.23 ± 0.08, 0.43 ± 0.03 and 0.41 ± 0.04 for 200, 225 and 250 W in Sn-AlN/Cu structure, which also demonstrate the AlN nanoparticles can decrease the growth rate, to retard the growth of nanothin Cu_6Sn_5 films. Al_2O_3 nanoparticles as additives into Sn-0.3Ag-0.7Cu/Ni-Cu structure (Tikale and Prabhu, 2020), can retard the IMC growth from 4 to 11 μm after reflow soldering. Combining our research about the nanothin Cu_6Sn_5 film, the nanoparticles can be used as the barrier for elements diffusion to control the IMC growth:

Figure 10 Schematically illustration of IMC growth mode

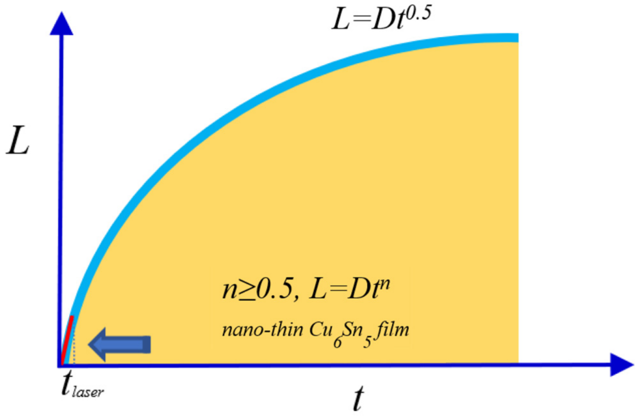

Source: Authors' own work

$$L = Dt^n \tag{4}$$

where L is the IMC thickness, D is the diffusion coefficient, t is the heating time and n is the reaction constant.

4. Conclusions

The present study appears to be the first study to experimentally demonstrate the formation of nanothin Cu_6Sn_5 films on the Cu substrates with laser heating in Sn/Cu and Sn-AlN/Cu structures. The conclusions can be drawn as follows:

- The thickness of Cu_6Sn_5 film increased from 635.6 to 890.9 nm and 524.2 to 792.3 nm for Sn/Cu and Sn-AlN/Cu structures with the increase of laser power from 200 to 250 W for 2 s heating time. The increase of laser power and laser heating time can improve the atoms diffusion to enhance the Cu_6Sn_5 thickness.
- The diameters of Cu_6Sn_5 grains can also be enhanced with the increase of laser power and heating time. The diameters of Cu_6Sn_5 grains in Sn/Cu structure are all over 1000 nm, for Sn-AlN/Cu structure, the diameters are 752.8 and 909.9 nm with 200 W and 2 s/3 s.
- The growth rate of Cu_6Sn_5 film in Sn/Cu structure is obviously higher than that in Sn-AlN/Cu structure; moreover, the value of reaction constant n for both structures is significantly larger, more than 0.5, and even up to about 1.

References

Abdullah, M.A. and Idris, S.R.A. (2021), "Effect of Sn-Cu solder alloy onto intermetallic formation after laser soldering", *Proceeding of International Conference in Mechanical Engineering Research*, pp. 869-880.

Gusak, A.M., Tu, K.N. and Chen, C. (2020), "Extremely rapid grain growth in scallop-type Cu_6Sn_5 during solid-liquid interdiffusion reactions in micro-bump solder joints", *Scripta Materialia*, Vol. 179, pp. 45-48.

Hu, X.W., Xu, H., Chen, W.J. and Jiang, X.X. (2021), "Effects of ultrasonic treatment on mechanical properties and microstructure evolution of the Cu/SAC305 solder joints", *Journal of Manufacturing Processes*, Vol. 64, pp. 648-654.

Huan, P.C., Tang, X.X., Sun, Q., Akira, K., Wang, X.N., Wang, J., Wang, J.L., Wei, X. and Di, H.S. (2022), "Comparative study of solder wettability on aluminum substrate and microstructure-properties of Cu-based component/aluminum laser soldering joints", *Materials & Design*, Vol. 215, p. 110485.

Kim, H.K. and Tu, K.N. (1996), "Kinetic analysis of the soldering reaction between eutectic SnPb alloy and Cu accompanied by ripening", *Physical Review B*, Vol. 53 No. 23, pp. 16027-16034.

Kunwar, A., An, L.L., Shang, S.Y., Råback, P., Ma, H.T. and Song, X.G. (2020), "A data-driven framework to predict the morphology of interfacial Cu_6Sn_5 IMC in SAC/Cu system during laser soldering", *Journal of Materials Science & Technology*, Vol. 50, pp. 115-127.

Li, M.L., Gao, L.L., Zhang, L., Long, W.M., Zhong, S.J. and Zhang, L. (2021), "Interfacial evolution of pure Sn solder bearing silicon carbide nanowires under isothermal aging and thermal cycling", *Journal of Materials Research and Technology*, Vol. 15, pp. 3974-3982.

Liu, W., Wang, C., Sun, L. and Tian, Y.H. (2010), "Effect of protection atmosphere's temperature on morphology of Au-Sn IMCs in laser reflowed micro-solder Joints", *11th International Conference on Electronic Packaging Technology & High Density Packaging*, *IEEE*.

Liu, Y., Pu, L., Yang, Y., He, Q., Zhou, Z., Tan, C., Zhao, X., Zhang, Q. and Tu, K.N. (2020), "A high-entropy alloy as very low melting point solder for advanced electronic packaging", *Materials Today Advances*, Vol. 7, p. 100101.

Liu, Y.X., Shi, X.Y., Ren, H.X., Cai, J., Zhao, X.C., Tan, C.W. and Tu, K.N. (2021), "Surface diffusion controlled reaction in small size microbumps", *Materials Letters*, Vol. 284, p. 129036.

Nishikawa, H. and Iwata, N. (2015), "Formation and growth of intermetallic compound layers at the interface during laser soldering using Sn-Ag-Cu solder on a Cu pad", *Journal of Materials Processing Technology*, Vol. 215, pp. 6-11.

Sun, L., Chen, M.H., Zhang, L. and Xie, L.S. (2019), "Effect of addition of CuZnAl particle on the properties of Sn solder joint", *Journal of Materials Processing Technology*, Vol. 278, p. 116507.

Tikale, S. and Prabhu, K.N. (2020), "Development of low-silver content SAC0307 solder alloy with Al_2O_3 nanoparticles", *Materials Science and Engineering: A*, Vol. 787, p. 139439.

Vianco, P.T., Kilgo, A.C., McKenzie, B.M., Grant, R.L. and Williams, S. (2022), "Interface embrittlement between 63Sn-37Pb solder and Au layer-part 1: physical metallurgy of liquid-state and solid-state reactions", *Journal of Electronic Materials*, Vol. 51 No. 11, pp. 6431-6453.

Wang, J.H., Xue, S.B., Liu, L., Zhang, P. and Nishikawa, H. (2022), "Three-dimensional interface and property of SnPb solder joint under extreme thermal shocking", *Science and Technology of Welding and Joining*, Vol. 27 No. 3, pp. 186-196.

Xiong, M.Y., Zhang, L., Sun, L., He, P. and Long, W.M. (2019), "Effect of CuZnAl particles addition on microstructure of Cu/Sn58Bi/Cu TLP bonding solder joints", *Vacuum*, Vol. 167, pp. 301-306.

Yao, P., Li, X., Liang, X.B., Yu, B., Jin, F.Y. and Li, Y. (2017), "A study on interfacial phase evolution during Cu/Sn/Cu soldering with a micro interconnected height", *Materials Characterization*, Vol. 131, pp. 49-63.

Zhang, L. and Liu, Z.Q. (2020), "Inhibition of intermetallic compounds growth at Sn-58Bi/Cu interface bearing CuZnAl memory particles (2-6 μm)", *Journal of Materials Science: Materials in Electronics*, Vol. 31 No. 3, pp. 2466-2480.

Zhang, L., Long, W.M. and Zhong, S.J. (2021), "Effect of thermal cyclic loading on stress-strain response and fatigue life of 3D chip stacking structure", *Chinese Journal of Mechanical Engineering*, Vol. 34 No. 1, p. 115.

Corresponding author

Zhang Liang can be contacted at: zhangliang2022xm@163.com